3D Modeling of Void Nucleation and Initial Void Growth due to Tin Diffusion as a Result of Electromigration in Polycrystalline Lead-Free Solders

by

Deepak Karunakaran

A Thesis Presented in Partial Fulfillment
of the Requirements for the Degree
Master of Science

Approved July 2016 by the
Graduate Supervisory Committee:

Yang Jiao, Chair
Nikhilesh Chawla
Jagannathan Rajagopalan

ARIZONA STATE UNIVERSITY

August 2016

ABSTRACT

Electromigration (EM) has been a serious reliability concern in microelectronics packaging for close to half a century now. Whenever the challenges of EM are overcome newer complications arise such as the demand for better performance due to increased miniaturization of semiconductor devices or the problems faced due to undesirable properties of lead-free solders. The motivation for the work is that there exists no fully computational modeling study on EM damage in lead-free solders (and also in lead-based solders). Modeling techniques such as one developed here can give new insights on effects of different grain features and offer high flexibility in varying parameters and study the corresponding effects. In this work, a new computational approach has been developed to study void nucleation and initial void growth in solders due to metal atom diffusion. It involves the creation of a 3D stochastic mesoscale model of the microstructure of a polycrystalline Tin structure. The next step was to identify regions of current crowding or 'hot-spots'. This was done through solving a finite difference scheme on top of the 3D structure. The nucleation of voids due to atomic diffusion from the regions of current crowding was modeled by diffusion from the identified hot-spot through a rejection free kinetic Monte-Carlo scheme. This resulted in the net movement of atoms from the cathode to the anode. The above steps of identifying the hotspot and diffusing the atoms at the hot-spot were repeated and this lead to the initial growth of the void. This procedure was studied varying different grain parameters. In the future, the goal is to explore the effect of more grain parameters and consider other mechanisms of failure such as the formation of intermetallic compounds due to interstitial diffusion and dissolution of underbump metallurgy.

ACKNOWLEDGMENTS

I express my gratitude to my advisor Dr. Yang Jiao, for his continuous guidance throughout the project. I appreciate the motivation, encouragement and the ideas he provided to help me perform the challenging research in this project. I thank my parents for their continuous support and love throughout my life.

I would like to thank my committee members, Dr.Nikhilesh Chawla and Dr.Jagannathan Rajagopalan for agreeing to serve on the committee and the feedback on the research. I would like to sincerely thank all the people I have cited in my references and other researchers in the field of microelectronics packaging from whom I received knowledge and inspiration throughout my research.

Last but not least, I would like to convey thanks to all the members of the Complex Materials Group - Yaopengxiao Xu, Shaohua Chen, Hechao Li, and Liang Long for their support from the beginning, in helping me fix issues in the code and also in the form of modeling ideas.

TABLE OF CONTENTS

LIST OF TABLES

LIST OF FIGURES

Figure Page

CHAPTER 1: INTRODUCTION

Ever since the time when the first integrated circuits became commercially available, EM has been a hot topic of research among investigators in the semiconductor industry and the academia. Even after half a century the problem of EM failures still persists though it has been largely been controlled. The adoption of new lead-free alloys whose EM performance has not been well researched and the use of smaller semiconductor devices resulting in higher current density are the two key challenges that are faced in the reliability of microelectronics packaging today. There has been significant work done on EM damage characterization through various experimental techniques such as X-ray Tomography [1][2]. In this research an attempt is made to model the void nucleation due to current crowding in a purely stochastic microstructure through microstructure evolution modeling with a goal to gain insight into various grain features that may affect the void formation.

In microelectronics packaging, EM has been the most persistent reliability concern [3]. It has severely reduced the life of Integrated Circuits by causing a loss of connection. EM is caused by electron wind force resulting in atomic migration. It can be described as the mass transport of atoms due to momentum transfer with electrons. It is imperative to take into account several different mechanisms such as the diffusion mechanisms and effect of current and heat etc. to study and understand the effect of EM. In alloys, phase segregation and other effects can reduce the lifetime of joints [4].

In this research an attempt is made to study the nucleation of the void at the hot spot through a coupled kinetic Monte Carlo- finite difference scheme and visualize the 'mass transport of atoms' that results in EM void nucleation and growth.

1.1 Black's Equation

Black's Equation is a mathematical model that is used to predict for the median time to failure of a semiconductor circuit due to EM.

$$\frac{1}{MTF} = AJ^2 exp - \emptyset/KT \qquad [5]$$

where
MTF = median time to failure in hours.
A = a constant which contains a factor involving the area
J = current density in amperes per square centimeter
$\emptyset$ = activation energy in electron volts
K = Boltzman's constant
T = film temperature in degrees Kelvin

The Black's equation articulates that the time to failure is inversely proportional to the square of the current density. The square relation is a matter of debate and many researchers use a value between 1 and 2. The value of this exponent is based on the underlying mechanism that explains the dominant phase of EM lifetime. If the exponent is close to 1 it indicates that the lifetime is dominated by the void growth mechanisms and a value close to 2 indicates that void nucleation will dominate [6]. The time to failure increases with the activation energy of the active mechanism and the decreases with increasing temperature. In this work we take into consideration grain boundary diffusion

of metal atoms during the simulation since it is the lower activation energy mechanism. The Black's equation provides a relationship between different parameters and EM lifetime but it does not provide any information about the underlying mechanisms. In order to have a more thorough understanding of the actual mechanisms, more sophisticated models is required that take into consideration the fundamental physics of the process.

1.2 Flip Chip Technology

Flip-chip (or controlled collapse chip connection) is an interconnection technology that has advantages over other packaging methods in terms of performance and cost. In a flip-chip the length of interconnections between chip and substrate is reduced by using solder bumps on the die and it involves the minimum length of electrical connections. The flip chip is called so because the active side of the chip is facing downwards. The chip is flipped over and aligned with landing sites on the substrate and reflowed in a reflowing oven. Flip-chip interconnects form the electrical and mechanical connections between IC and the package. One of the main functions of the flip-chip solder joint is to form the mechanical connection between the chip and the substrate. The under bump metallurgy (UBM) provides the right combination of properties to form a solderable surface on the die. The formation of the intermetallic compounds depends on the thickness of the UBM. Thicker layer would lead to a delayed formation of intermetallic compounds since the UBM acts as the diffusion barrier and delays the formation these compounds that may affect the mechanical integrity of the solder.

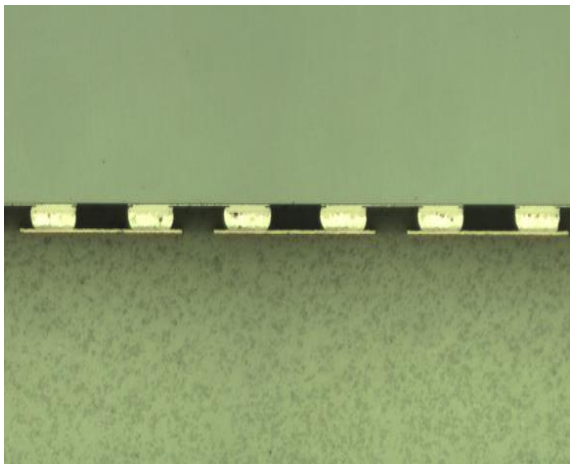

Fig. 1. Pb-Free solders for Flip-Chip interconnects.

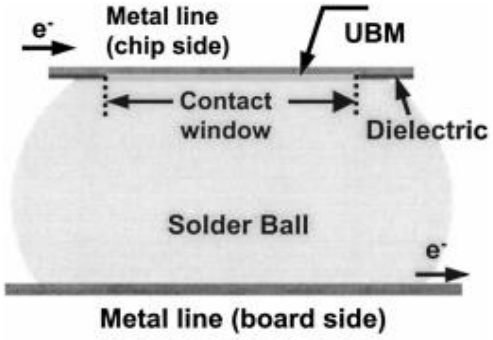

Fig. 2. Schematic of a flip-chip solder bump [7]

1.3 Lead-Based And Lead-Free Solders.

The use of Lead-containing solders has reduced drastically in the electronic packaging industry due to environmental and health concerns and is being replaced by Lead-free solders whose primary component is Tin [9]. The use of lead-based solders has offered several advantages. Lead provides good ductility in Tin-Lead solders [10]. The wetting angle of Lead alloys on Copper is much lesser than that of pure Tin on Copper [11]. Eutectic Tin-Lead solder has a low reflow temperature since it has a low eutectic point. Lead-based solders are popular due to its low cost and its mechanical properties [12]. The combination of Lead and Tin offer provide favorable properties for the above-mentioned reasons.

Most Lead-free alloys are Tin based since Tin has many favorable properties such as it can wet a wide range of substrates. The use of Tin also has challenges which include

whisker growth and the anisotropic nature of Tin due to its body centered tetragonal structure causing problems during thermal cycling. Whisker growth which is not observed in lead-Tin solders can cause electrical shorts in the PCB. [13]

The main problems that are faced because of replacing Lead-based solders is that there is an established knowledge about the manufacturing techniques, metallurgy, and reliability of Lead based solders. The use of Tin-based solders is relatively a new area and has poor field data. For a successful substitution of the former using the latter more research is required to understand the different mechanisms. This is one of the motivations of this work.

1.4 Modes of Damage in Lead-Free Tin Based Solders

In Lead-free Tin solders, EM induced damage may be classified into modes. Mode-I damage occurs through the self-diffusion of Tin atoms through the vacancy mechanism. This results in a pancake type void formation. Mode I operates at a higher temperature because the vacancy diffusion mechanism requires a higher activation energy. The presence of intermetallic compounds provides a weak surface and voids may form at the interface between the intermetallic compound and the solder. [14]

Mode-II damage has lower activation energy since it occurs through interstitial diffusion mechanism that can occur at a lower temperature. It involves interstitial diffusion of the metals in the under bump metallurgy that are usually copper or nickel [14]. In other words, the governing mechanism is temperature dependent. Pancake void formation occurs at higher temperatures and consumption of the UBM (under bump metallurgy) occurs at lower temperatures.

The mechanism also strongly depends on the alignment of Tin grains in the solder microstructure.

Tin has a body-centered tetragonal structure [14]. The lattice parameters being a=b= 5.83 Å and c= 3.18 Å [15]. There is faster diffusion of Copper and Nickel along ‘c’ axis due to this reason. Researchers have reported that the room temperature diffusivity of copper in Tin is 500 times faster along the ‘c’ axis than along ‘a’ or ‘b’ axis. [15]. When electron

flow in the solder microstructure is not aligned with the Tin ‘c’ axis, the dominant mechanism is Tin self-diffusion that has higher activation energy. [16]

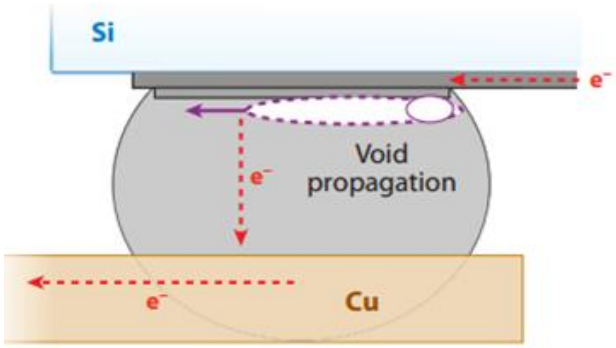

Fig. 3. A cross section of a solder joint with a pancake void at the cathode side of solder [5].

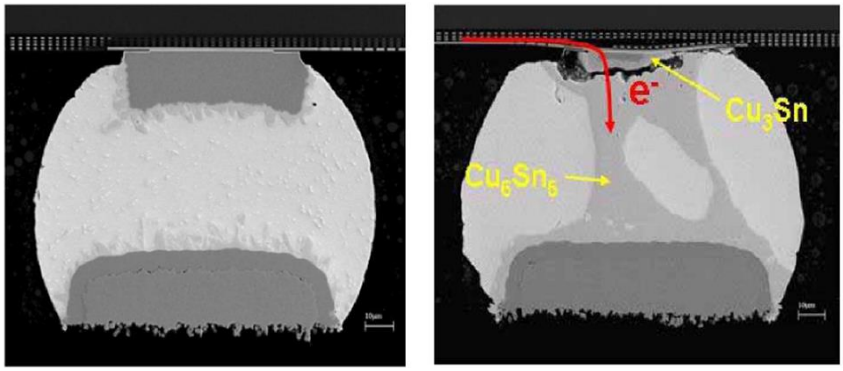

Fig. 4. Micrographs of crossections Sn-3.5Ag solder bump before and after current stressing [16].

1.5 Effect of thickness of UBM on failure mechanism

The UBM serves many purposes. It forms the electrical connection between the die and the solder bump. It limits the diffusion by acting as a barrier between the bump and the

die. In flip chip solders the major cause of EM failure is current crowding. The mechanism depends on the thickness of the under bump metallurgy. A thick UBM will lead to the distribution of the current over a large area. Such a configuration will lead to a near uniform current density in the solder structure. In this case current crowding is close to insignificant in the solder. When there is a thin UBM the current crowding effect is significant in the solder. The void initiates at the point with the maximum current density and the thin UBM us fully consumed. This region is very close to the entrance of the solder.

The void nucleated grows along the solder intermetallic surface as the intermetallic is brittle. This eventually results in the formation of a pancake void. To summarize the effect of the cooper under bump metallurgy it can be said that in case of a thick UBM the current crowding takes places in the UBM which starts dissolving into the solder and in thin solder joints the void nucleation starts at the region of the peak current density.

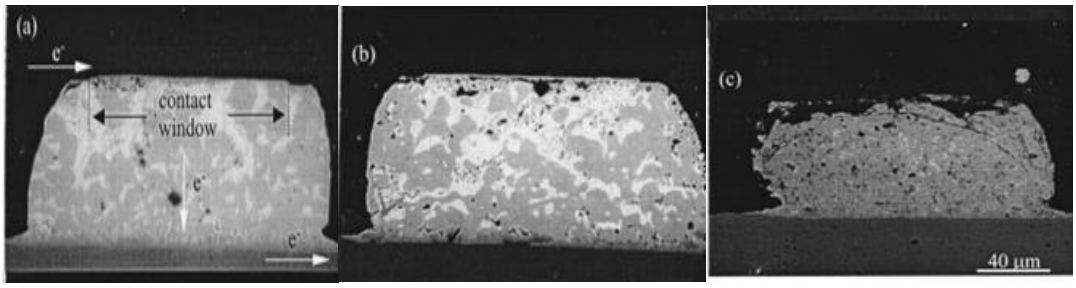

Fig. 5. The different stages of void formation and propagation due to current stressing in a flip-chip solder joint. [11]

CHAPTER 2: MOTIVATION AND OBJECTIVES

2.1 Motivation of the Study

Due to environmental and health concerns there is a drive towards eliminating the use of lead in microelectronic packaging industry. It is crucial to understand material properties of lead-free solder for a successful substitution of lead-based solders. Another challenge in the reliability of interconnects is the increased miniaturization of semiconductor devices [8] causes the higher temperature in the metal interconnects, typically resulting in EM failures.A technique is developed and applied to study EM-induced void nucleation through a coupled Kinetic Monte-Carlo and finite difference scheme. There is an effort made to study EM void nucleation in a mesoscale model of the metallic polycrystalline solder. We take into consideration the different physical mechanisms that lead to the formation of the void to create the model. Rejection-free Kinetic Monte Carlo simulations have been used to model the diffusion of the atoms. A finite difference method is used to identify the regions of high current (hotspots).

2.2 Objectives of the Research

The first objective was to create a 3D mesoscale model representative of a polycrystalline grain structure. Secondly, the structure created was converted to a dual phase structure of grain and grain boundary phase. This implies that all the grains have similar properties and cannot be distinguished. Thirdly, the application of a finite difference scheme to identify the hot-spots. Fourthly, the Kinetic Monte-Carlo diffusion that leads to the nucleation of the voids. Finally, the goal is to understand the effect of different grain

parameters on the diffusion path taken by individual atoms and void characteristics of the solder interconnect.

CHAPTER 3: CREATION OF THE STRUCTURE

The solder structure created in all the cases in this work involves a 100x100x100 system which is a cube of 10^6 voxels. The edge length of the cube is considered 50 μm. The initial structure was created by choosing 'N' random nucleation sites (picked by the C++ random number generator) and letting the grains grow from these nuclei until they impinge and fill the cubical space. In the figure 6 and 7, N is equal to 100 grains. For all the initial simulation work 'N' was chosen to be 100 grains. In later part of the research different values of "N" were tried to study the effect of grain size on void formation and diffusion of atoms. The structure obtained was polycrystalline. All the grains were of random shapes and sizes.

For the diffusion of Tin atoms, there is no role played by the anisotropic structure of Tin (Tin has a body-centered tetragonal structure with c axis shorter than the 'a' and 'b' axis which effects Copper/ Nickel diffusion rates). The diffusion of Tin occurs by vacancy mechanism as opposed to interstitial diffusion for Copper and Nickel atoms.

Having made this assumption the mesoscale structure was converted to a binary structure with grain and grain boundary being the two phases. This implies that all the grains have a similar effect on Tin diffusion. Figure 6 shows the 100 random nuclei generated by the C++ random number generator and on the right the 100 grains that were grown from the nuclei. Figure 7 shows the same structure converted to a two phase structure of grain and grain boundary

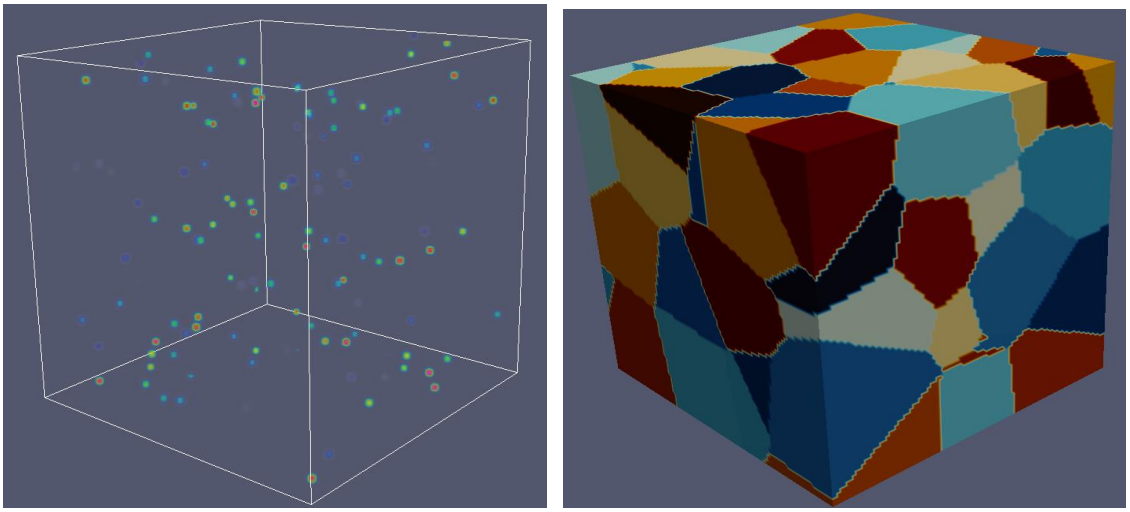

Fig. 6. Nucleation points in space and 100 grain mesoscale model of the initial structure.

.

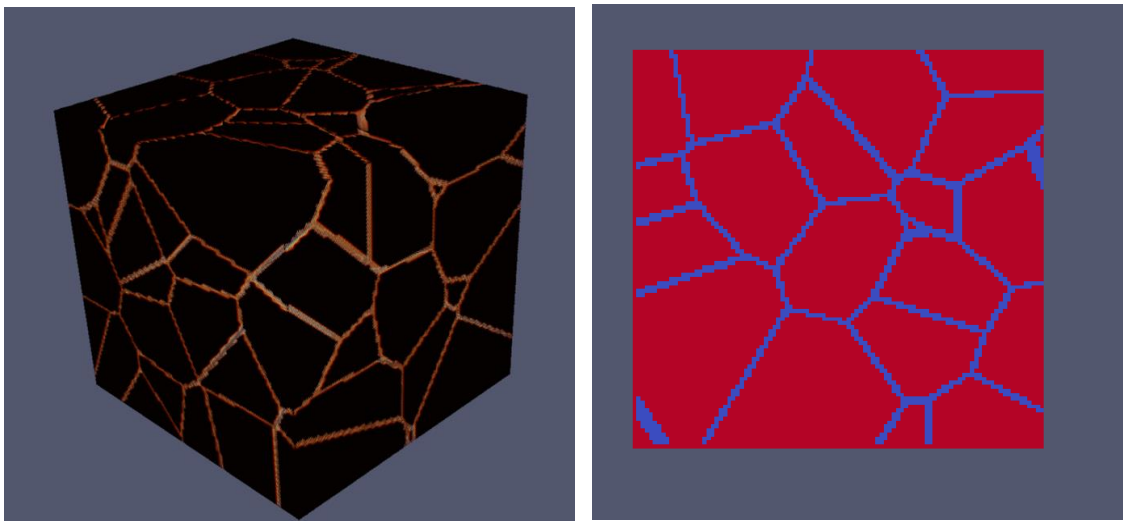

(a) (b)

Fig. 7. The polycrystalline structure converted to a binary structure with grain and grain boundary being the two phases (a) 3D structure –black=grain, gold= grain boundary. (b) 2D slice- red= grain, blue= grain boundary.

3.1 Assumptions of the Model

One important assumption that is made is that grain structure is static. There is no effect of Joule-heating on the mesoscale structure. Some researchers [8] have shown that the current-crowding effect leads to an increase in temperature those results in coarsening of grain structure. No chemical reactions and mechanical stresses were also considered. The focus of the study is to model the net flow of atoms due to EM, the creation of voids near the vicinity of current crowded regions at the cathode end and the accumulation of atoms at the anode end. The work focuses on Mode I damage and thus also doesn't consider the formation of intermetallic compounds.

CHAPTER 4 MODELLING DIFFUSION

4.2 Grain Boundary Diffusion

The mechanism of diffusion is considered is grain boundary diffusion. Grain boundaries provide for a faster medium of diffusion as they are regions of defects and also, in general, the activation energy for grain boundary diffusion is always less than the activation energy for lattice diffusion. Defining the grain boundary is a very critical component. Once the grain structure was created the grain boundary was defined by borrowing one voxel from either side of the grains along the common separating interface between the grains. This definition was maintained throughout the structure to obtain a uniform two layer grain boundary diffusion path. Certain region where the thickness of the grain boundary was higher was at triple points.

4.3 Kinetic Monte-Carlo Diffusion

The kinetic Monte Carlo method has been employed extensively in materials modeling. It is a very popular technique for studying transport (diffusion on surface and in materials)[17], reaction kinetics, and other diffusion-related problems. For creating models that involve fundamental stochastic processes, Kinetic Monte Carlo Simulations provide a very simple yet effective tool [20]. Though the Fick's laws provide a deterministic equation for diffusion the movement of individual atoms in a lattice is random [20]. Therefore the Kinetic Monte Carlo simulations are used to model the diffusion of Tin atoms in this work. The diffusion of individual Tin atoms are stochastic in nature since the influence of electron flow is considered, it favors the net movement of atoms from the cathode to the anode.

4.3.1 The Rejection Free Kinetic Monte Carlo Diffusion

The Rejection free Kinetic Monte Carlo technique is similar to rejection sampling technique in statistics and is used here to simulate the diffusion-time evolution of the system. It is explained using the illustration provided. This does not fully represent the actual system (explained in the next section) where a few aspects are slightly different, such as the direction of the current.

Individual atoms are allowed to jump one pixel for each attempt, meaning the atoms can jump to one of the 7 first-order nearest grain boundary pixels (in 2 dimensions). The jumping event is a pixel exchange that takes place between the initial state and the final state. The atom may jump to a grain boundary pixel based on a random number generated. This is to ensure that all the neighboring grain-boundary pixels have an equal chance of getting picked. This does not imply that there is an equal probability of exchange with all of the neighboring pixels, as the individual probability of a successful transition will vary based on the location of the neighboring pixel with respect to the diffusing pixel and the defined current vector.

In the figure 8 the atom ‘X’ under consideration may exchange pixels with its nearest neighbor pixels that are grain boundaries which are numbered 1-4. In this case we assume that the direction of electron flow is from the cathode to the anode and perpendicular toh the grain surfaces. The maximum probability of transitioning is to pixel 2 (as it is in line with the direction of the current) and minimum for pixel 4.

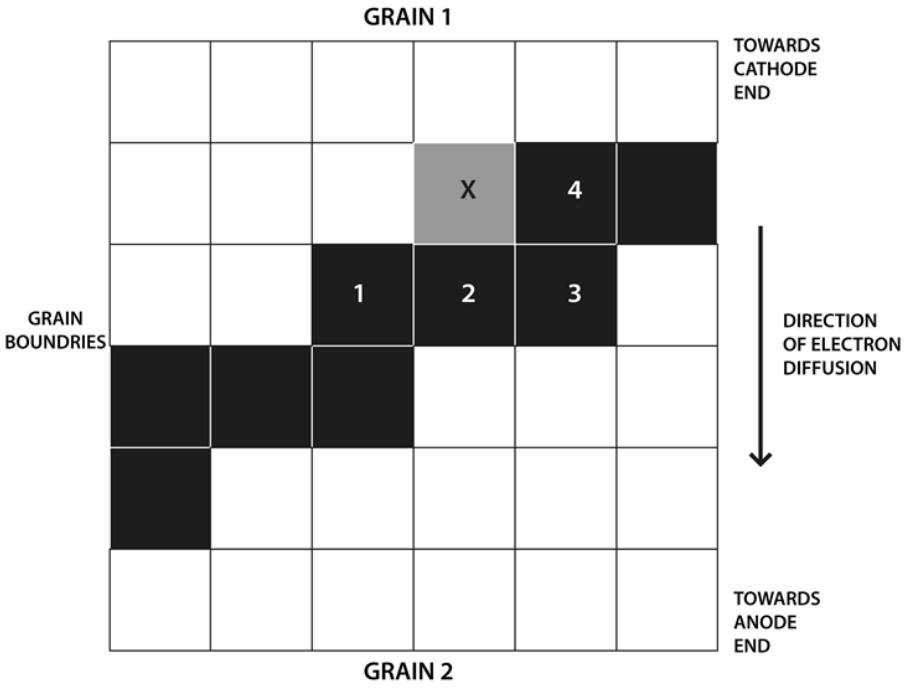

Fig. 8 A figure to illustrate a system that is undergoing rejection free Kinetic-Monte Carlo evolution in 2D. The atom under consideration is marked 'X' and the numbered black pixels are the states that can exchange with 'X'.

The transfer probability is proportional to the dot product of current vector and the jump vector (the vector between the initial and final states.) The probability that the system jumps into state 'i' is proportional to 'Γ_i' where 'Γ_i' is the calculated dot product. The transition probability is calculated for all the possible transitions between the diffusing atom and the possible final states.

The probability of jumping is scaled by a normalizing factor 'Γ_{total}' where 'Γ_{total}' is the sum of all the individual probabilities of atom transitions to each of its grain boundary voxels. This is done so as to obtain a number between '0' and '1'. This number is compared to a random number generated between 0 and 1. If the probability is greater than the random number generated then we accept the move else we reject it. Some

moves will be accepted and the others rejected and this process continues for a certain fixed number of Monte-Carlo time-steps.

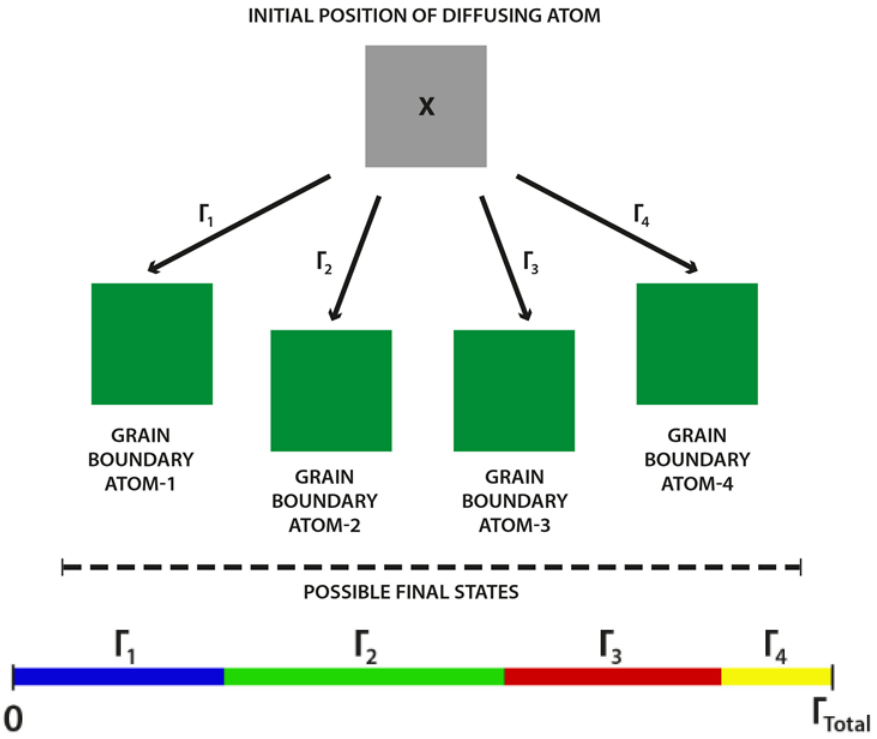

Fig. 9 The atom under consideration at each 'Monte-Carlo time-step' can exchange pixels with one of several states, The exchnage probabilty rates for atom 'X' from figure 8 and different final states are shown on the scale. The probability of jumping into state i is proportional to length of Γ_i.

4.3.2 Diffusion Process

The diffusion process is similar to the explanation provided for the 2D case with some additional factors that are considered. From the chosen hot-spot atoms diffuses simultaneously. This takes place step by step for a total of 1000 Monte Carlo attempts. This number was chosen as a significant amount of diffusion could be visualized in the different cases (covered in the next chapter). The atoms are allowed to jump to one of 26

nearest grain boundary voxels (in three dimensions).

The probability of success depends on many factors. Firstly, the initial state, the set of final states and the current vector. Secondly, the number of grain boundary voxels surrounding a given grain voxel. More grain boundaries means a given grain can jump in one of the many possible voxels hence the probability of success increases. Since we define the diffusion to be grain boundary based. The success rate for the transition out of 1000 attempts depends on the grain structure. At the most fundamental level it depends on the neighbors surrounding the diffusing atom. In general a system having high grain boundary to grain voxel ratio will have high transition probability.

We keep track of the movement of atoms in a separate array. This is done so as to visualize the diffusion path of individual atoms. The spread of the final location of the diffusing atoms depend on the number of grains in the structure. There is more spread when there are more grains as this result in more grain boundaries in the system. When there are fewer grain boundaries there is a more direct path to diffuse to the anode end of the system. When there is a higher ratio of grain boundary to grain there is a greater probability for the transfer to successfully occur. This is the reason why there is a greater chance of success when there is more number of grains.

4.4 Modeling Atomic Diffusion

Two approaches were attempted to model the diffusion of atoms due to EM. The first one was to model the diffusion of vacancies, since the Tin atoms diffused through vacancy diffusion. The second approach was to model the actual diffusion of Tin atoms. The

reason a second approach was needed was to overcome the shortcomings of the first approach. The second approach involves a better implementation of the different mechanisms involved in EM.

4.4 First Approach: Vacancy Diffusion Method

The initial formulation to model EM induced damage was based on the the diffusion of vacancies. This was considering that diffusion of vacancies and atoms are equal and opposite events.

In this model an initial concentration of vacancies was provided in the system that was distributed randomly within the grain boundaries. Vacancies were allowed to diffuse under the rejection free Kinetic Monte Carlo process. Before the simulation an approximately equal concentration of vacancies at the cathode and anode end (and throughout the system) was observed. After the simulation there was a high concentration of vacancies at the cathode and low at the anode end. The preferential clustering was observed at the cathode end in the 3D model can be explained by current-bias that causes the vacancies to diffuse toward the cathode end, forming clusters.

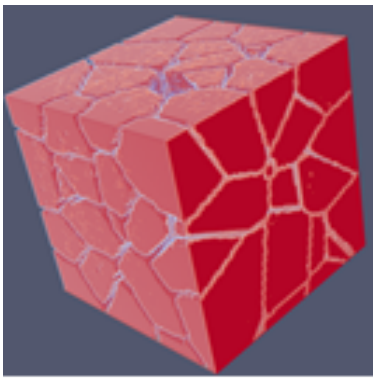

Fig. 10. Void formation at the cathode end. Red indicates Grain. White/transparent indicates grain boundary. The large transparent area on top is the void formation at cathode end (Top end).

4.4.1 Failure of the Model

This formulation does not produce the desired features that would be typically seen on the SEM images of solder microstructure after an EM failure. This is because in this model the effect of current crowding was not considered. The EM effect was maximum at the hotspots were the current crowding took place, in this model it was not possible to consider the hotspots and initiate the diffusion at this point since the vacancies are spread throughout the system.

4.5 Second Approach: Diffusion of Tin Atoms

This formulation involved diffusion of Tin atoms instead of vacancies. In this model the hot-spots or regions of highest current crowding or temperature were identified. This was done by solving for the voltage distribution in the system after applying a fixed voltage at the edge of the system in cathode end where the current enters the system. After identifying the hotspots the diffusion of Tin atoms was initiated from these spots. The atoms diffuse from the hotspots and migrate toward the anode end due to current biased diffusion. It was also possible to track the movement of individual atoms as they diffuse towards the anode. The formation of the voids was also captured.

4.5.1 Identifying the Hotspots

Hotspots are regions where current crowding takes place. This results in a higher temperature in these regions as compared to the rest of the solder structure. This part of the code was written in MATLAB 8.1 2013a. Central difference method was implemented to find the solution the laplacian for the voltage distribution. This was done

with a mesh size of (100x100x100). The objective of the program is to solve for the steady state voltage distribution in a region 1<=x<=100, 1<=y<=100, 1<=z<=100.

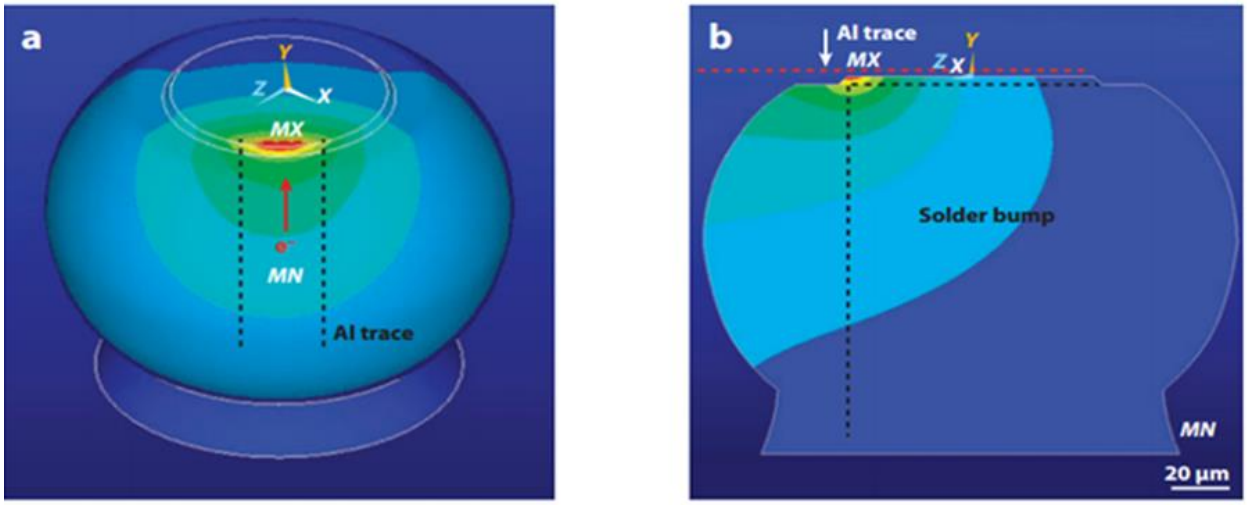

Fig. 11. Simulated heat map of current distribution showing current crowding in flip-chip solder joints. The maximum value of the current density is at the point where the current enters the solder [8].

Uniform voltage is applied at an edge at the cathode side from where the current enters and all other sides are maintained at '0' volts. At any iteration, the value of voltage is updated as the average of voltages of 8 nearest neighbors, until between consecutive iterations the tolerance in error between iterations reaches 0.01 V.

When the simulation was over the atoms containing the maximum values of the voltage was identified. Theses atoms were allowed to diffuse through 1000 time steps through the Kinetic Monte-Carlo Algorithm. The default current vector that was considered was from the cathode edge (where the current enters) to the diagonally opposite edge at the anode end.

4.6 Effect of Grain Size on EM

Since grain boundary diffusion is the primary mechanism, the number of grains in the system is an important parameter that affects EM void formation characteristics. A system having a large number of grains would provide an easy path for the grains to diffuse. This is clearly observed when comparing the diffusion results for the 20-grain and 1000-grain system (in the results section).

In the 1000-grain system a large volume fraction of the structure is occupied by the grain boundary voxels. This is illustrated in figure 12. This means that the diffusing metal atoms have a greater access to the grain boundary and are able to diffuse to the anode faster. This was observed as expected in the simulations and is reported in the results section. In order to observe the effect of grain size, different systems were created where the number of grains was varied between 20 grains to 1000 grains, the hotspots were identified and the kinetic Monte-Carlo diffusion was allowed to take place. All grains are created by random numbers provided by C++. The diffusion path in each case tracked and visualized.

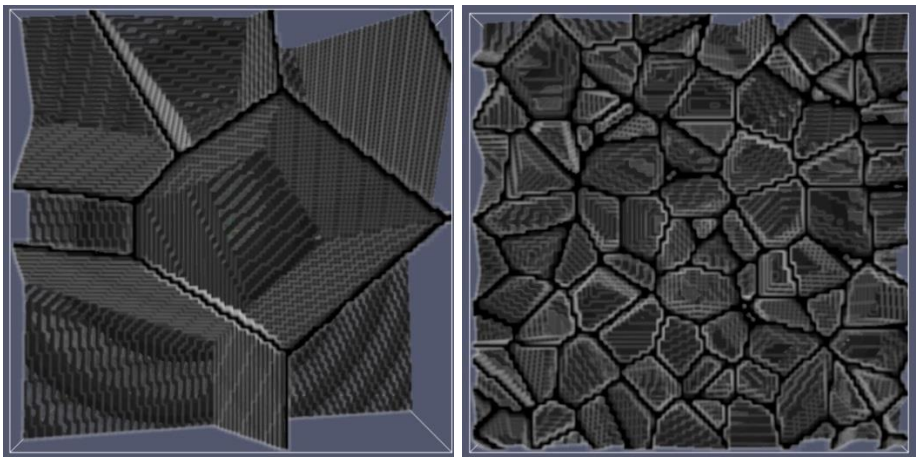

Fig 12. Grain Boundaries in a 20 grain and a 1000 grain structure.

CHAPTER 5: RESULTS

5.1 Statistics of Grain Distribution for Structure having 10-1000 Grains

To understand the size distribution of the stochastically created microstructures basic statistics is done on the structures created. The grain size is measured by assuming that the grain shape is spherical and by counting the number of enclosed voxels by each grain.

For different grain systems the mean, median, standard deviation and range of grain size is reported. The median grain size decreases when the number of grains increased since the total volume is the same for all the cases. The variance of grain volume increases with decreasing grain size. This implies that when the number of grains is small there are very large and small grains and vice versa. Table 1 helps us understand the size distribution of the grains that were generated.

Parameter	20 Grains	50 Grains	100 Grains	500 Grains	1000 Grains
Range of Grain Size (μm)	10.28-28.74	11.55-24.04	6.41-16.96	3.57-10.84	2.85-8.90
Mean Grain Size (μm)	22.85	16.82	13.36	7.81	6.20
Median Grain Size (μm)	18.14	13.93	13.05	6.08	4.70
Standard Deviation	23.09	15.27	10.11	7.67	6.07

Table 1.Statistics of the grains generated.

5.2 20-Grain System

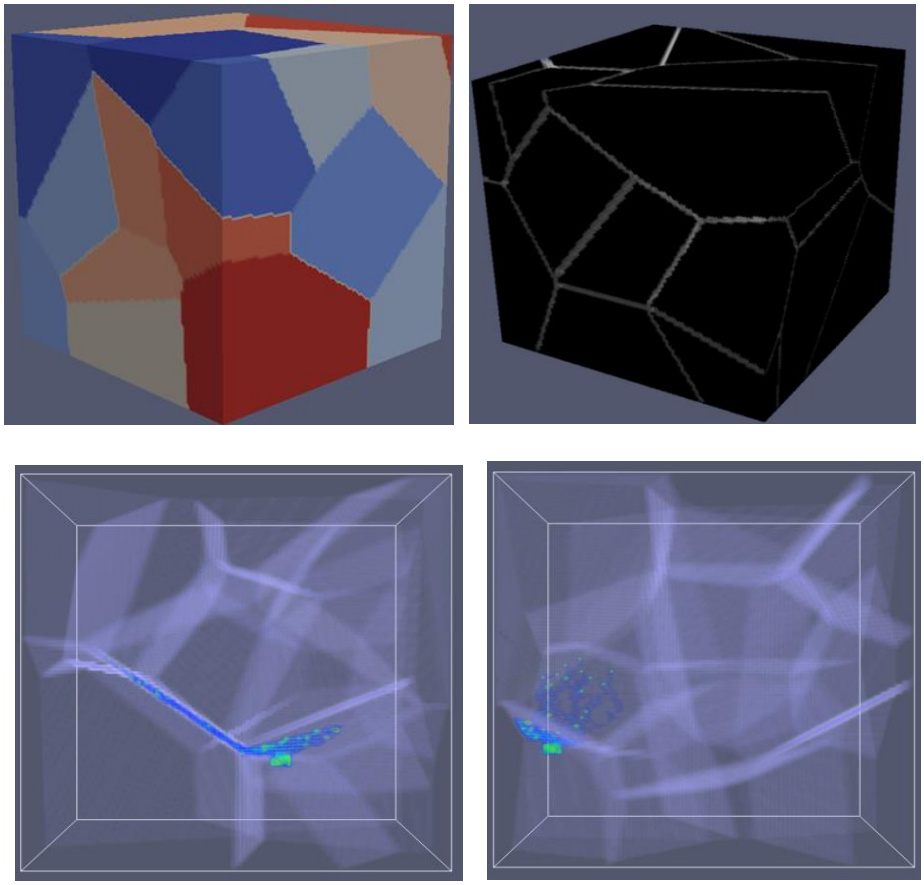

Fig. 13. Simulation results for a 20 grain system. From top clockwise. (1) initial grain structure (2) 3D binary structure (3) Front view at the end of diffusion process. (4) Side view at the end of diffusion process. (3) and (4) show void formation near the cathode end in green, blue lines are the diffusion path of induvidual Tin atoms migrating from the hot-spot, induividual green dots are final position of the atoms.

5.3 50-Grain System

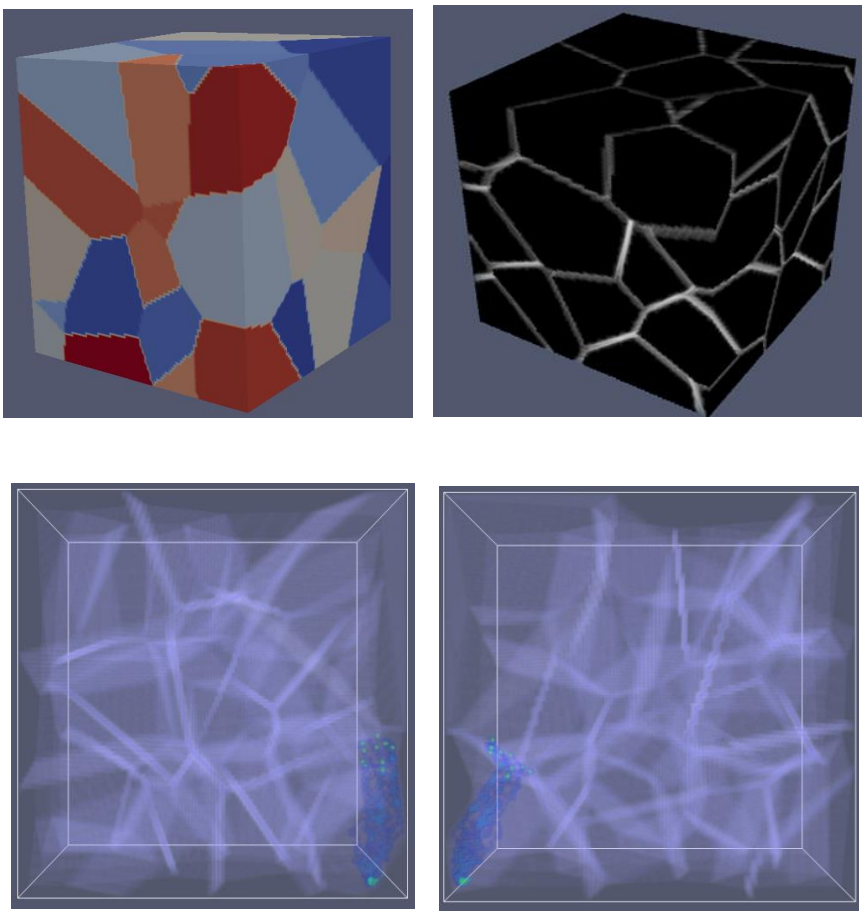

Fig.14. Simulation results for a 50 grain system. From top clockwise. (1)Initial grain structure (2) 3D binary structure (3) Front view at the end of diffusion process. (4) Side view at the end of diffusion process. (3) and (4) show void formation near the cathode end in green, blue lines are the diffusion path of induvidual Tin atoms migrating from the hot-spot , induividual green dots are final position of the atoms.

5.4 100-Grain System

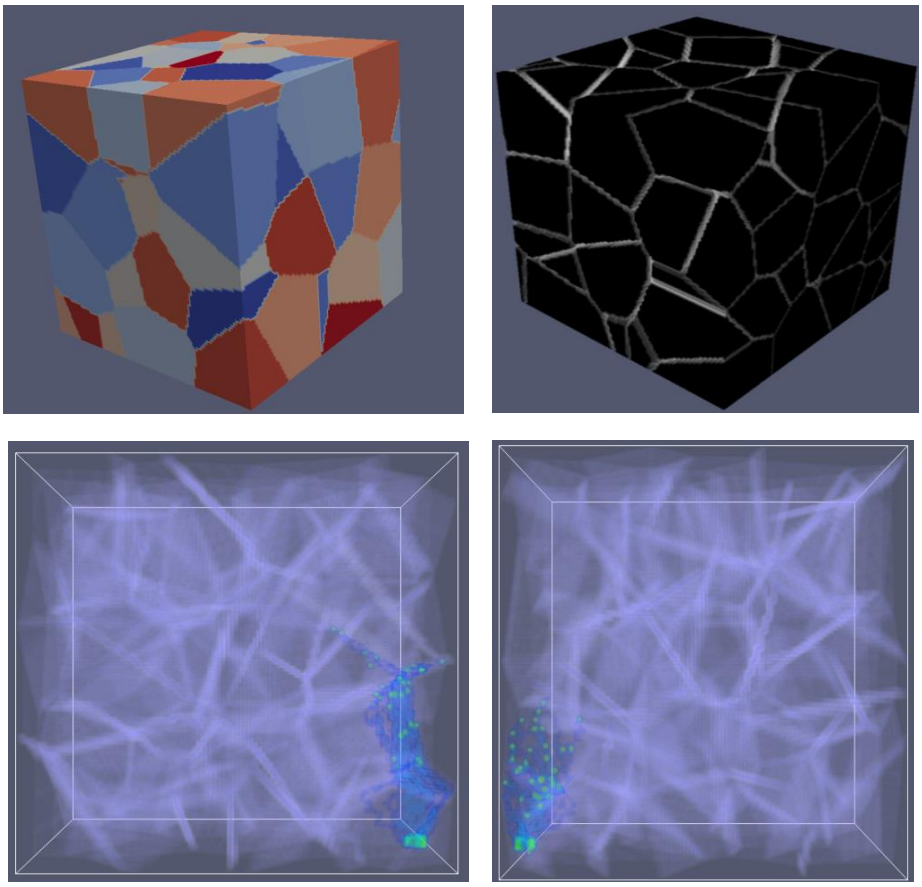

Fig 15. Simulation results for a 100 grain system. From top clockwise. (1)Initial grain structure (2) 3D binary structure (3) Front view at the end of diffusion process. (4) Side view at the end of diffusion process. (3) and (4) show void formation near the cathode end in green, blue lines are the diffusion path of induvidual Tin atoms migrating from the hot-spot , induividual green dots are final position of the atoms.

5.5 500-Grain System

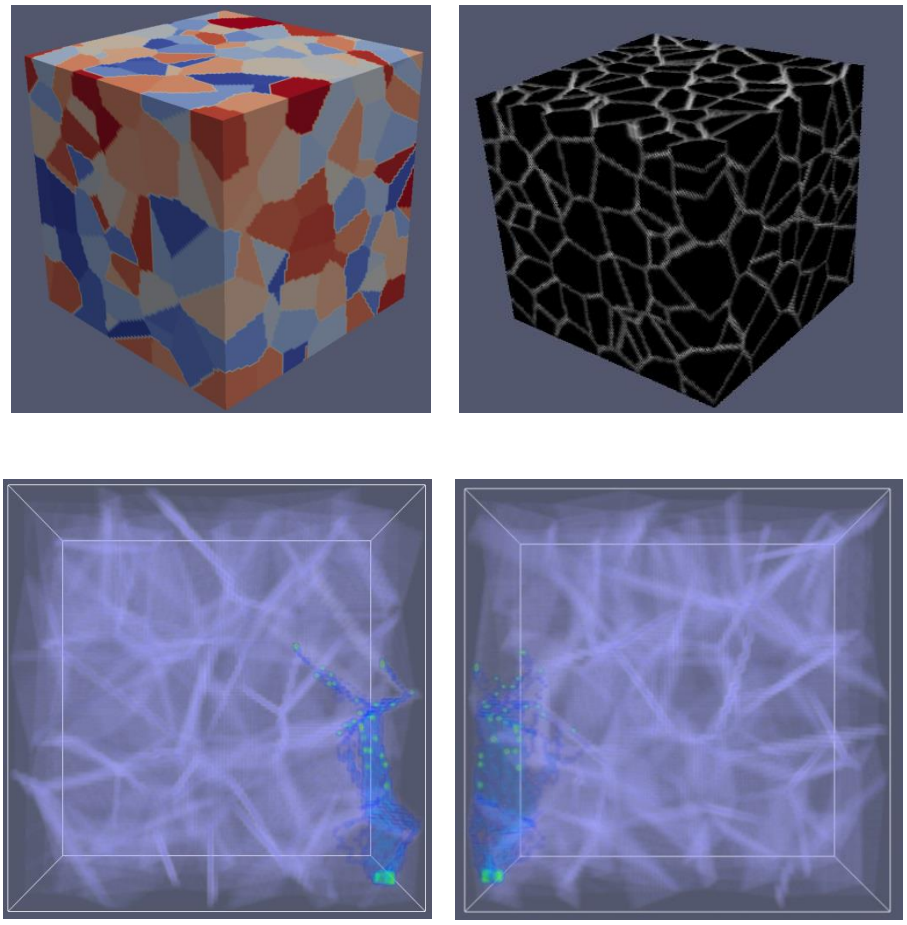

Fig 16. Simulation results for a 500 grain system. From top clockwise. (1)Initial grain structure (2) 3D binary structure (3) Front view at the end of diffusion process. (4) Side view at the end of diffusion process. (3) and (4) show void formation near the cathode end in green, blue lines are the diffusion path of induvidual Tin atoms migrating from the hot-spot , induividual green dots are final position of the atoms.

5.6 1000-Grain system

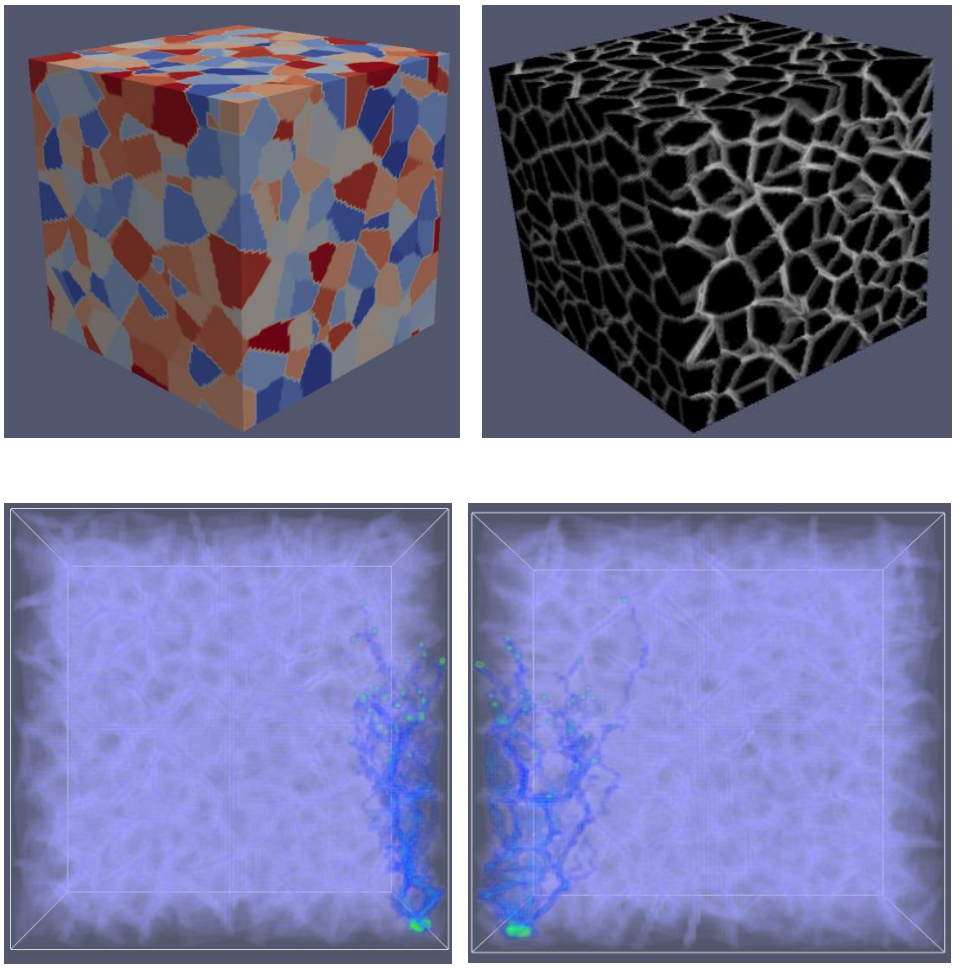

Fig 17. Simulation results for a 1000 grain system. From top clockwise. (1)Initial grain structure (2) 3D binary structure (3) Front view at the end of diffusion process. (4) Side view at the end of diffusion process. (3) and (4) show void formation near the cathode end in green, blue lines are the diffusion path of induvidual Tin atoms migrating from the hot-spot, induividual green dots are final position of the atoms.

5.8 Comparison of Diffusion Behavior of Tin Atoms in a 20 Grain, 100 Grain, 500 Grain, 1000 Grain System

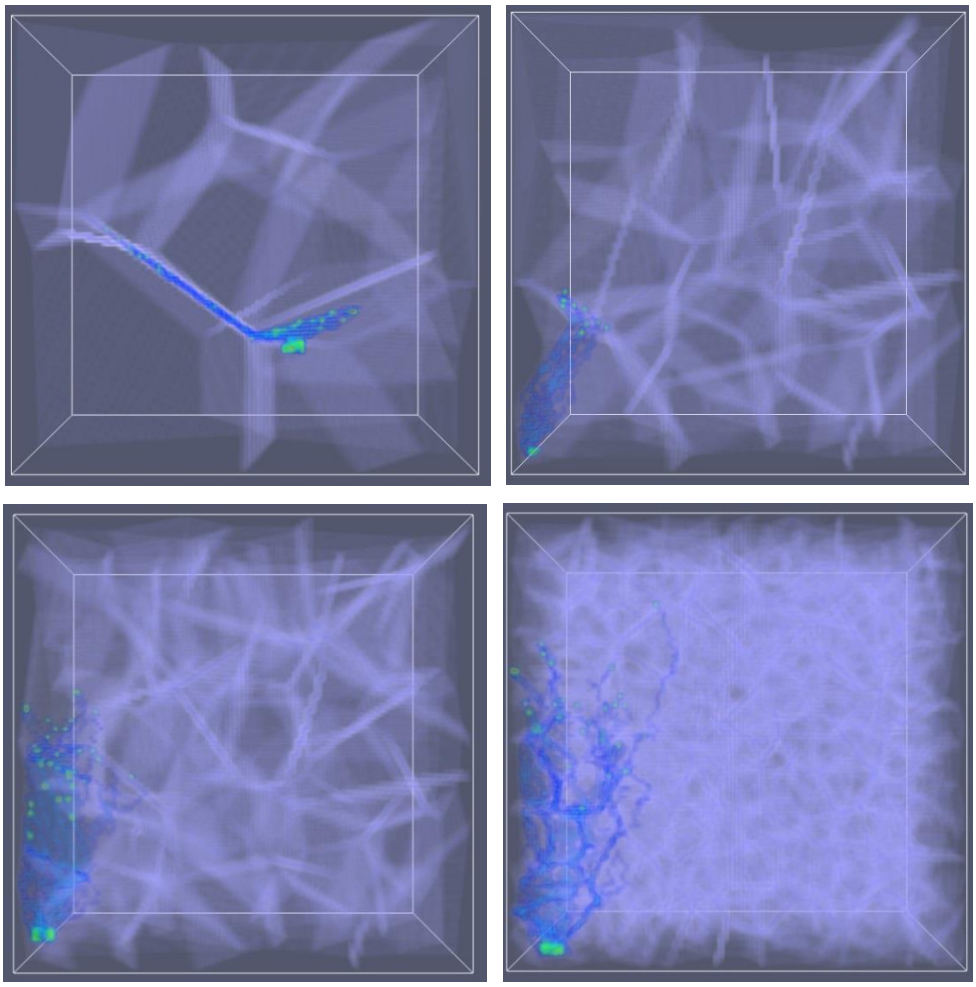

Fig. 18. Comparing diffusion behavior in(clockwise from top left) in 20 grains, 50 grains, 100 and 1000 grains in a [100x100x100] space after 1000 time steps.

The blue region is the diffusion path of atoms migrating from the hot-spot. It is observed from Figure 18 that a system that has a higher number of grains will have more successful Tin atom diffusion jumps towards the anode as indicated by the greater range of the blue region. This can be explained by the fact that having more grains will result in more channels for the atoms to diffuse towards the anode. It is also observed that in a 20-

grain system the atoms are trapped in a grain boundary that is near parallel to the solder surface and is hence not able to migrate towards the anode.

5.9 Effect of Grain Boundary Angle

Many studies [18][19] have shown that the grain boundary angle plays a significant role in EM performance. One study [18] mentions that the lifetime of an interconnect can be increased by having high angle twin boundaries in tin- based solders.

In order to study the effect of grain boundary angle different structures were created by tweaking an existing structure to result in a high angle grain boundary having the same grain configuration as the original. The amount of tin-atom diffusion was observed to be different in the case of high and low angle grain boundaries. More atomic-diffusion was seen in the case of low-angle grain system than a high-angle grain system for the same configuration of grains.

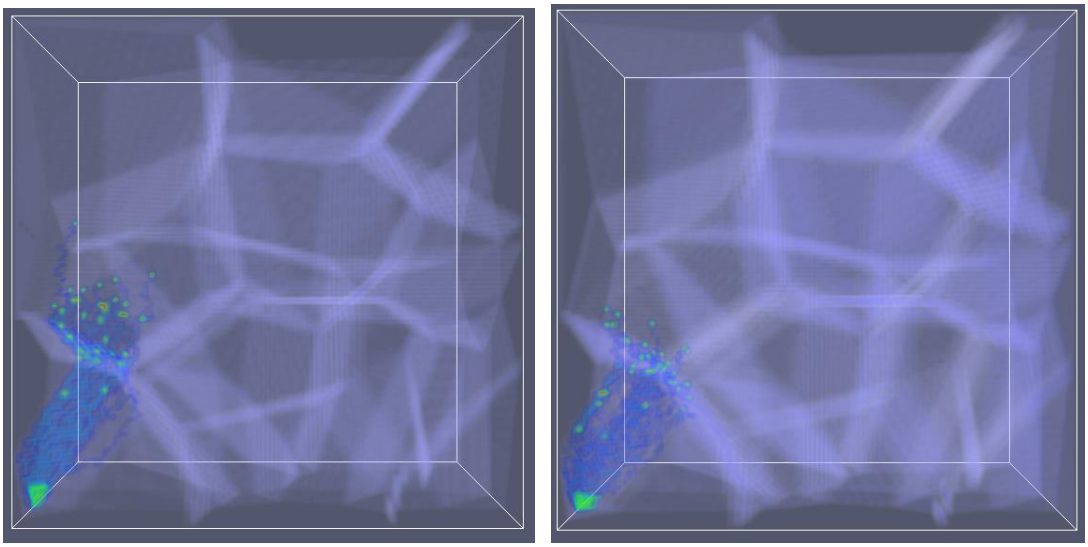

Fig. 19. Low angle grain boundary system(left) and high angle grain boundary system(right) in a configuration having 30 grains.More atomic diffusion observed on the low angle grain boundary system.

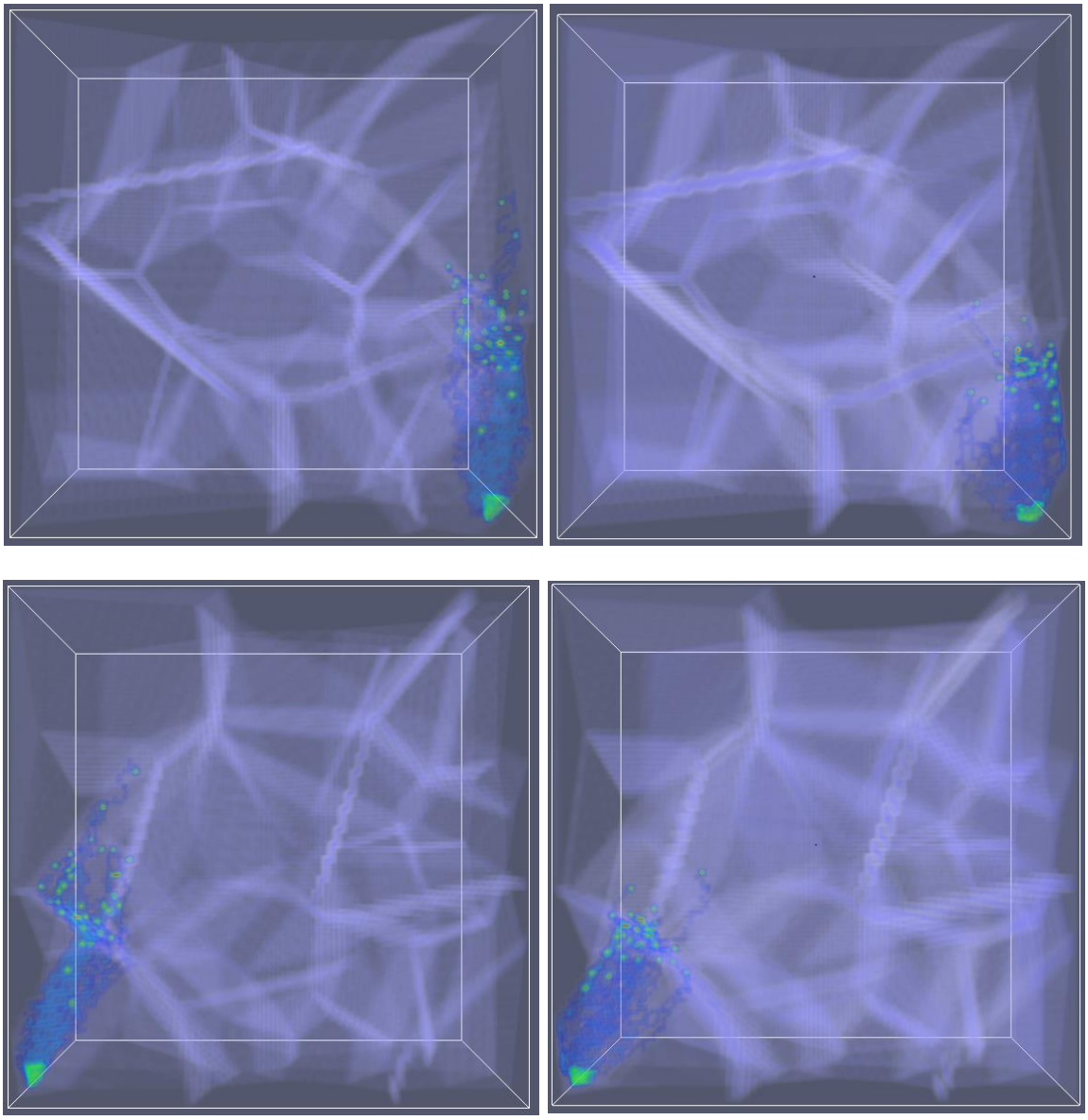

Fig 20.Front view(images on top) and side view(images in the bottom) of the same grian configuration having 60 grains. Low angle grain boundary system(images on the left) and high angle grain boundary system(images on the right) in a sysrtem . More atomic diffusion observed on the low angle grain boundary system. Void formation was observed in the cathode end (bottom) in all four cases.

5.7 Quantifying Movement of Atoms

Number of Grains	Average Displacement of atoms towards Anode (in μm)	Average Distance Travelled by atoms(in μm)
20 grains	8.81	9.23
50 grains	13.81	14.42
100 grains	15	16.63
500 grains	16.04	17.47
1000 grains	17.91	19.05

Table 2. Net diffusion distance of atoms for 20-1000 grains after 1000 Monte Carlo steps.

Number of Grains	Type of Grain Boundary	Average Displacement of atoms towards Anode(in μm)	Average distance Travelled by atoms(in μm)
30 grains	Low angle	24.11	26.71
	High angle	16.95	18.35
60 grains	Low angle	25.62	27.54
	High angle	17.47	18.44

Table 3. Net diffusion distance of atoms for in a 30 and 60 grain system, to compare low-angle and high-angle boundary diffusion after 3000 Monte Carlo steps.

5.10 Tracking Diffusion from more than one Hotspot

In all the previous cases we looked at diffusion from a single hot-spot. In practice the diffusion takes place simultaneously from multiple regions. With the objective of visualizing the diffusion process from two current-crowded regions, figure 20 was generated for a 100 grain system (left) and a 1000-grain (system).

It is noticed that as the atoms attempt to migrate from the cathode to the anode there is some convergence in the paths of the atoms. From the results of this simulation, it is expected that as we take into consideration a higher number of hotspots there is a strong likelihood of the diffusion paths of atoms converging. This interference in the path of the movement of individual atoms may result in the interaction between diffusing atoms and affect the net migration of the atoms.

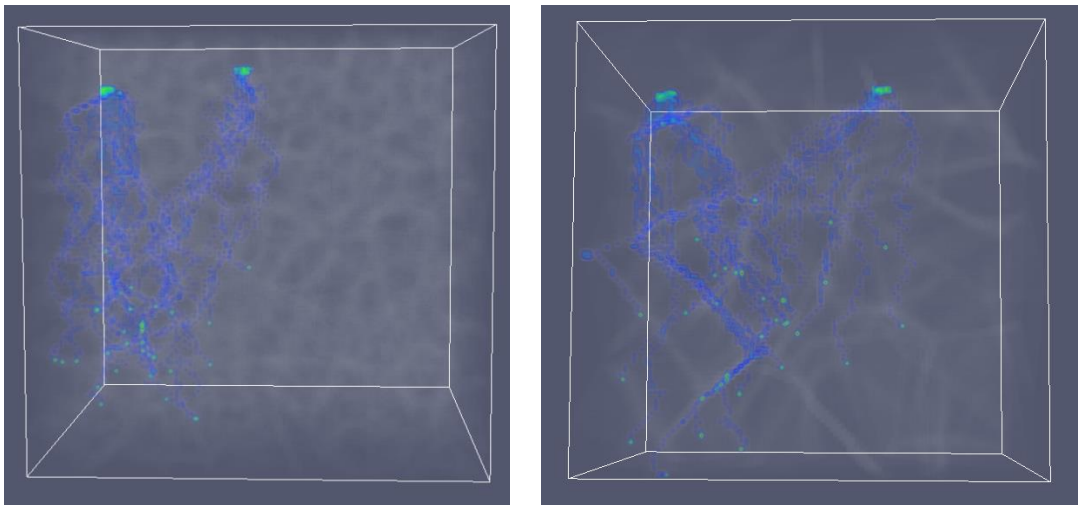

(a) (b)

Fig 21.Tracking diffusion from two hotspots.(a)1000 grains (b) 100 grains.The images show two voids formed by simultaneous diffusion of Tin atoms.

5.11 Effect of Direction of Current on Diffusion Path of Atoms

In the present implementation of the model it is possible to vary the direction of the current vector and see the corresponding effect on the diffusion path of the atoms. The convention used for the axes are defined first. The perpendicular line form the anode to the cathode (as shown in the figure 22) is defined as 'x' axis (used as the baseline) and the direction perpendicular to the 'x' axis in the plane of the paper is the 'y' axis. $\vec{\imath}$ and $\vec{\jmath}$ are unit vectors along 'x' and 'y' axis.

The simulation is performed varying the direction of the current starting with $\vec{\imath}$ direction and moving towards $\vec{\jmath}$ direction. Four different directions were attempted for the current vector, they were- i, $\vec{\imath} + \vec{\jmath}$, $\vec{\imath} + 2\vec{\jmath}$ and $\vec{\imath} + 3\vec{\jmath}$.

The results obtained from the simulation are as expected and are visualized in the figure 22. The net diffusion distance of the atoms from cathode to anode decreases with increasing angle. As the direction of the current was varied from 0° ($\vec{\imath}$) to 72.5° ($\vec{\imath} + 3\vec{\jmath}$), the diffusion of atoms was favored in that respective direction.

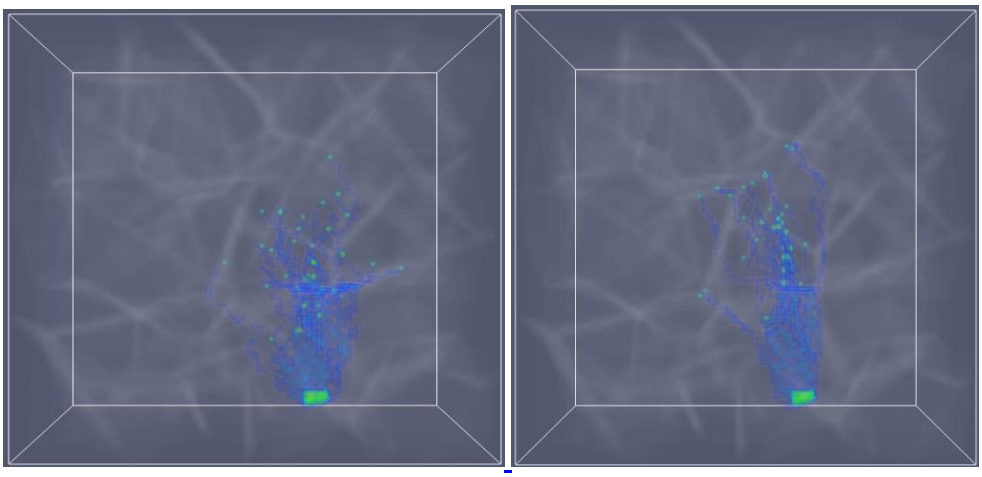

Fig 22. The simulated diffusion path for current vector of direction $\vec{\imath}$ (left) and $\vec{\imath} + \vec{\jmath}$ (right).

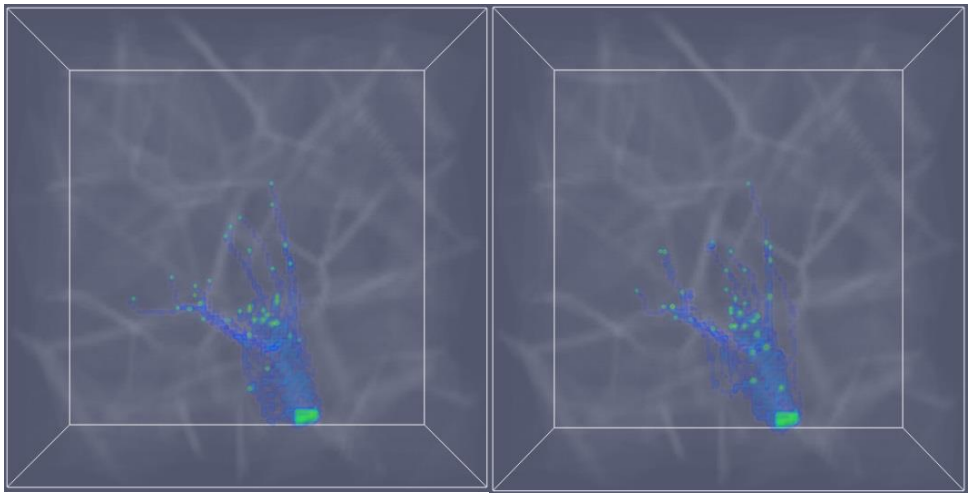

Fig 23. The simulated diffusion path for current vector of direction $\vec{\imath} + 2\vec{\jmath}$ (left) and $\vec{\imath} + 3\vec{\jmath}$ (right).

CHAPTER 6: CONCLUSION

The purpose of this work was to (1) create a mesoscale model of EM void formation and visualize the diffusion of Tin atoms during the process of EM (2) vary general parameters in the system and observe the corresponding effect on diffusion and (3) compare the EM life performance with some previously conducted experimental studies.

A computational framework has been developed to model EM void nucleation through a coupled kinetic Monte-Carlo diffusion and finite difference scheme and this is modeled by considering grain-boundary diffusion. This model can be used to compare Mode I EM damage and diffusion behavior for different configurations of grains. In this study, two different grain parameters were varied and their effects were qualitatively and qualitatively studied. The two-grain parameters are grain size and grain boundary angle. From the simulation results obtained it was concluded that larger grain size and high grain boundary angles improved EM life. This is in congruence with experimental studies conducted. Other parameters such as the direction of the current vector were varied and the simulation results were visualized. The model created is flexible; any new mechanism that is unaccounted for in the current model can be implemented on top of the existing scheme. Visualizing the diffusion path of the atoms is a very powerful tool. A movie of diffusion of Tin atoms from the hot-spot and the void nucleation process was created for different scenarios (different grain parameters). This helps in visualizing the diffusion of Tin atoms that takes place during current stressing in different cases. More insights can be gained by considering more mechanisms and studying the simulation results.

CHAPTER 7: FUTURE WORK

7.1 Improving the Model

As mentioned earlier the model has a few assumptions. Eliminating these assumptions involves complications but will lead to more practical results. Coarsening of grains takes place due to increased temperature because of Joule Heating. A 3D simulation through finite elements analysis can be carried out to model the steady state temperature distribution. This can be coupled with Potts model which is commonly used to model recrystallization and grain growth. Combining these two methods it would be possible to model the coarsening of grains that takes place.

It would be more challenging to accurately model Mode II damage that involves diffusion of copper and Nickel from the under bump metallurgy through interstitial diffusion. This involves chemical reactions and formation of intermetallic compounds such as Cu_6Sn_5 and Cu_3Sn and also a weak surface on which void grows. The mechanical integrity of the solder and the composition changes plays a key role in this mode of failure.

7.2 Exploring More Scenarios: Modeling the Effect of Anisotropic Grain Structures on Diffusion

The current model has been tested on several structures that were isotropic in nature. Going one step further, the current implementation can be used to model grain structures that have a certain orientation such as elliptical close-packed grains. Modeling this scenario can provide insights into the effect of specific orientations in EM damage. In the current implementation, it is possible to create different kinds of structures just by

feeding the coordinates of the nuclei into the system the prewritten algorithm will be able to produce the corresponding structures. This assumes that growing uniformly in all the directions will result in the intended structure.

Another interesting case that can be explored is having fine-grained and coarse-grained region in a single system. The fine grained region would contain more grain boundaries than a coarse-grained region. Theoretically such a structure would lead to accumulation of atoms at the transition region when the diffusion is from a fine-grained region into a coarser grained region. On the other hand, when atoms diffuse from a coarser to a fine grain size there should be voiding.

7.3 Machine Learning to Understand EM

The use of machine learning algorithms has been very limited in the field of material science considering the impact that it has had on other major fields such as medicine, physics, and biology. The use of supervised learning techniques can give us new hidden insights that are not so easily observed through traditional methods.

The use of these techniques can be used to understand 'trends' that favor void formation. The basic framework for the implementation would be as follows: Using historical data (data obtained through past simulations) a model can be trained under supervised learning technique such as neural network or random forest, with the void size as the outcome variable and the different predictors being grain size, grain distribution, the number of grains, grain orientation and possibly more.

Using this formulation it would be possible to identify the contribution or the statistical significance of different parameters to void formation. This can give an idea of the relative importance of different parameters to void growth.

REFERENCES

[1] Xie, H. X., et al. "Electromigration damage characterization in Sn-3.9 Ag-0.7 Cu and Sn-3.9 Ag-0.7 Cu-0.5 Ce solder joints by three-dimensional X-ray tomography and scanning electron microscopy." *Journal of Electronic Materials* 43.1 (2014): 33-42.

[2] Mertens, J. C. E., Kirubanandham, A., & Chawla, N. (2016). Electromigration mechanisms in Sn-0.7 Cu/Cu couples by four dimensional (4D) X-ray microtomography and electron backscatter diffraction (EBSD). Acta Materialia, 102, 220-230.

[3] Chen, C., & Liang, S. W. (2007). Electromigration issues in lead-free solder joints. Journal of Materials Science: Materials in Electronics, 18(1-3), 259-268.

[4] A. Lee, W. Liu, C. E. Ho, and K. N. Subramanian, J. Appl. Phys. 102, 053507 (2007)

[5] Black, James R. "Electromigration—A brief survey and some recent results." *IEEE Transactions on Electron Devices* 16.4 (1969): 338-347.

[6]De Orio, R. L., Hajdin Ceric, and Siegfried Selberherr. "Physically based models of electromigration: From Black's equation to modern TCAD models." *Microelectronics Reliability* 50.6 (2010): 775-789

[7] Yeh, E. C., Choi, W. J., Tu, K. N., Elenius, P., & Balkan, H. (2002). Current-crowding-induced electromigration failure in flip chip solder joints. *Applied physics letters*, *80*(4), 580-582.

[8] Chen, C., Tong, H. M., & Tu, K. N. (2010). Electromigration and thermomigration in Pb-free flip-chip solder joints. Annual Review of Materials Research, 40, 531-555

[9] Peercy, P. S. (2000). The drive to miniaturization. Nature, 406(6799), 1023-1026.

[10] Lin, J. A., Lin, C. K., Liu, C. M., Huang, Y. S., Chen, C., Chu, D. T., & Tu, K. N. (2016). Formation Mechanism of Porous Cu3Sn Intermetallic Compounds by High Current Stressing at High Temperatures in Low-Bump-Height Solder Joints. Crystals, 6(1), 12.

[11] Kim, H. K., Liou, H. K., & Tu, K. N. (1995). Morphology of instability of the wetting tips of eutectic SnBi, eutectic SnPb, and pure Sn on Cu. *Journal of materials research*, *10*(03), 497-504

[12] Wang, Mingna, et al. "Effect of Ag 3 Sn intermetallic compounds on corrosion of Sn-3.0 Ag-0.5 Cu solder under high-temperature and high-humidity condition." Corrosion Science 63 (2012): 20-28.

[13] Abtew, M., & Selvaduray, G. (2000). Lead-free solders in microelectronics. Materials Science and Engineering: R: Reports, 27(5), 95-141.

[14] Lu, Minhua, et al. "Effect of Sn grain orientation on electromigration degradation mechanism in high Sn-based Pb-free solders." Applied Physics Letters 92.21 (2008): 211909.

[15] Dyson, B. F., Anthony, T. R., & Turnbull, D. (1967). Interstitial diffusion of copper in tin. Journal of Applied Physics, 38(8), 3408-3408.

[16] Chao, B., Chae, S. H., Zhang, X., & Ho, P. S. (2007, April). Kinetic Analysis of Electromigration Enhanced Intermetallic Growth and Void Formation in Pb-Free Solders. In *Thermal, Mechanical and Multi-Physics Simulation Experiments in Microelectronics and Micro-Systems, 2007. EuroSime 2007. International Conference on* (pp. 1-8). IEEE.

[17]. Chatterjee, Abhijit, and Dionisios G. Vlachos. "An overview of spatial microscopic and accelerated kinetic Monte Carlo methods." *Journal of computer-aided materials design* 14.2 (2007): 253-308

[18] Wang, Yiwei, et al. "Effect of Sn grain structure on electromigration reliability of Pb-free solders." *Electronic Components and Technology Conference (ECTC), 2011 IEEE 61st*. IEEE, 2011.

[19] Galand, R., Arnaud, L., Petitprez, E., Brunetti, G., Clement, L., Waltz, P., & Wouters, Y. (2011, May). Grain boundary as relevant microstructure feature for electromigration in advanced technology studied by Electron BackScattered Diffraction. In Interconnect Technology Conference and 2011 Materials for Advanced Metallization (IITC/MAM), 2011 IEEE International (pp. 1-3). IEEE.

[20].Battaile, C. C. (2008). The kinetic Monte Carlo method: Foundation, implementation, and application. Computer Methods in Applied Mechanics and Engineering, 197(41), 3386-3398.